

ON DAVYDOV'S α -HELIX SOLITONS

J. M. HYMAN AND D. W. McLAUGHLIN

Research Group T-7
Los Alamos Scientific Laboratory
Los Alamos, New Mexico

A. C. SCOTT

Department of Electrical and Computer Engineering
University of Wisconsin
Madison, Wisconsin

Abstract. Numerical studies of Davydov's nonlinear dynamic model for the α -helix protein confirm his prediction of soliton formation. These solitons are robust, localized, dynamic entities that couple molecular (amide-I) vibrations to longitudinal sound waves; they may provide an efficient mechanism for energy transport in biological systems. Both the numerical studies and analytical computations show a threshold level of nonlinearity below which solitons will not form. A rough estimate indicates that this nonlinearity has the required order of magnitude.

1. INTRODUCTION

"How can energy be transmitted in biological systems?" This basic question was discussed in depth at a meeting of the New York Academy of Sciences in 1973, amid talk of a "crisis in bioenergetics."¹ A central issue in the "crisis" is that the attractive mechanism of energy transduction via excited molecular vibrations is presumed (on the basis of a *linear* dynamic analysis) to have an unacceptably short lifetime; but a potential resolution of this objection has been proposed by Davydov.² He suggests that the *nonlinear* character of interatomic forces (e.g., the hydrogen bond) can lead to the formation of

robust solitary waves (often called "solitons"³), which exhibit greatly increased radiative lifetimes and a correspondingly increased ability to transport energy over large distances.

As a specific context for the development of his idea, Davydov has concentrated on the α -helix protein and has chosen the relatively isolated amide-I (or C=O "stretch") vibration of the peptide group as the main "basket" in which energy is carried. According to a linear analysis, energy transported by this means should spread out from the effects of dispersion and should rapidly become disorganized and lost as a source for biological mechanisms. But in the nonlinear analysis of Davydov, propagation of amide-I vibrations is retroactively coupled to longitudinal sound waves of the α -helix, and the coupled excitation propagates as a localized and dynamically self-sufficient entity called a soliton. The amide-I vibrations generate longitudinal sound waves that in turn provide a potential well that prevents vibrational dispersion; thus the soliton holds itself together.

For such a coupled excitation to be viable, certain "threshold" conditions must be satisfied. The nonlinear coupling between amide-I vibrations and nonlinear sound waves must be sufficiently strong and the amide-I vibrations must be energetic enough for the retroactive interaction to "take hold." Below this threshold, a soliton cannot form and the dynamic behavior will be essentially linear. Above threshold the soliton is a possible mechanism for lossless energy transduction.

This chapter reports on a numerical study of Davydov's fundamental equations that confirms his analytical results. A sharp threshold between linear (dispersive) behavior and nonlinear (soliton) formation is clearly seen, and this threshold is related to fundamental physical parameters describing the α -helix protein. In Section 2 we describe for the general reader the basis for these numerical computations. To this end each term in Davydov's model is physically described with reference to the basic atomic structure. Section 3 displays our main numerical observations with emphasis on their physical significance. Finally we summarize our results and discuss some important open questions in this new area of *nonlinear biomolecular dynamics*. All mathematical discussions are presented in appendices, not because we feel that these are unimportant but to make the scientific logic of Davydov's theory as clear and as widely understandable as we can. This theory may, after, all, help to resolve the "crisis in bioenergetics."

2. DAVYDOV'S MODEL FOR α -HELIX PROTEIN

The atomic structure of α -helix protein is sketched (as a stereogram) in Fig. 1. The basic helix follows the sequence:



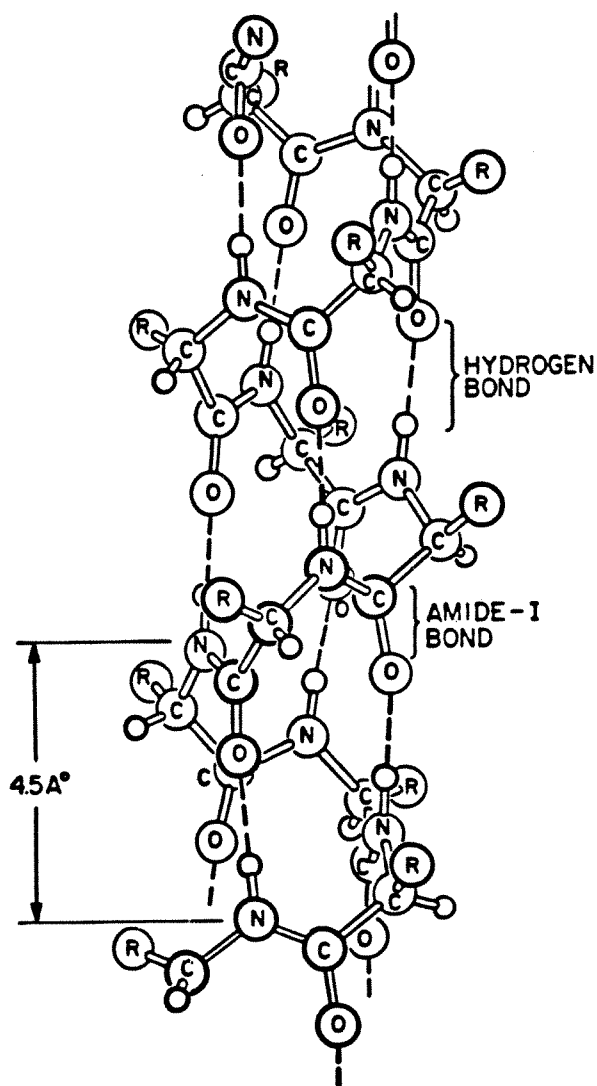
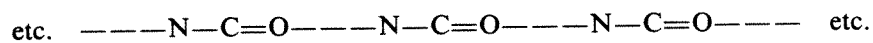


Figure 1. Stereogram of α -helix protein.

with a pitch of 5.4 Å. Superimposed on this basic structure are three "spines," which are almost longitudinal with the sequence:



where "O=C" represents the locus of the amide-I vibration and "O---N" is the longitudinal hydrogen bond that holds the structure in its helical form. Davydov's equations describe propagation along these three spines of amide-I

bond energy and longitudinal sound waves. Nonlinearity of the hydrogen bond leads to coupling of these two propagating systems and, if certain threshold conditions are satisfied, the formation of a soliton.

Let us begin by considering the equations that Davydov has derived to describe propagation along the three spines. From⁴ these are:

$$i\hbar \frac{da_{n\alpha}}{dt} = [\mathcal{E}_0 + W + \chi_1(\beta_{n+1,\alpha} - \beta_{n-1,\alpha})] a_{n\alpha} \\ - J(a_{n-1,\alpha} + a_{n+1,\alpha}) + L(a_{n,\alpha+1} + a_{n,\alpha-1}) \\ + \chi_2[\beta_{n+1,\alpha} a_{n+1,\alpha} - \beta_{n-1,\alpha} a_{n-1,\alpha} - \beta_{n\alpha}(a_{n+1,\alpha} - a_{n-1,\alpha})] \quad (1)$$

$$M \frac{d^2 \beta_{n\alpha}}{dt^2} - w(\beta_{n+1,\alpha} - 2\beta_{n\alpha} + \beta_{n-1,\alpha}) = \chi_1(|a_{n+1,\alpha}|^2 - |a_{n-1,\alpha}|^2) \\ + \chi_2[a_{n\alpha}^*(a_{n+1,\alpha} - a_{n-1,\alpha}) \\ + (a_{n+1,\alpha}^* - a_{n-1,\alpha}^*) a_{n\alpha}] \quad (2)$$

$$W \equiv \frac{1}{2} \sum_{n,\alpha} \left[M \left(\frac{d\beta_{n\alpha}}{dt} \right)^2 + w(\beta_{n\alpha} - \beta_{n-1,\alpha})^2 \right] \quad (3)$$

Broadly speaking, Eq. (1) describes the propagation of amide-I vibrations via dipole-dipole interactions and Eq. (2) represents the propagation of longitudinal sound. The total longitudinal sound energy is defined in Eq. (3). Each term, when individually considered, is quite plausible.

2.1. Subscripts

There are two subscripts to the dynamical variables, n and α . These run over the ranges:

$$n = -1, 0, 1, 2, \dots, n_{\max}$$

$$\alpha = 1, 2, 3$$

Thus n specifies a particular unit cell along a spine and α chooses a particular spine.

2.2. Bond Occupation Amplitude $A_{n\alpha}$

Consider Eq. (1) with the nonlinear coefficients χ_1 and χ_2 , the dipole-dipole coupling coefficients J and L , and the sound energy W set equal to zero. Then we have

$$i\hbar \frac{da_{n\alpha}}{dt} \doteq \mathcal{E}_0 a_{n\alpha} \quad (1')$$

In this equation

$$|a_{n\alpha}|^2 = a_{n\alpha} a_{n\alpha}^*$$

represents the probability of finding a quantum of bond energy \mathcal{E}_0 at unit cell n on spine α . If for the sum of such probabilities we have

$$\sum_{n, \alpha} |a_{n\alpha}|^2 = 1$$

a single quantum of amide-I bond energy is present on the helix.

Equation (1') is the quantum dynamical description of a simple oscillator. It says that the magnitude of $a_{n\alpha}$ remains constant and its phase progresses linearly with time as

$$a_{n\alpha}(t) = a_{n\alpha}(0) \exp\left(\frac{-i\mathcal{E}_0 t}{\hbar}\right)$$

From Ref. 5 $\mathcal{E}_0 \doteq 1650 \text{ cm}^{-1}$ in spectrographic units,* thus

$$\begin{aligned} \mathcal{E}_0 &= .205 \text{ eV} \\ &= 0.328 \times 10^{-19} \text{ J} \end{aligned}$$

2.3. Longitudinal Displacement $\beta_{n\alpha}$

Consider Eq. (2) with the nonlinear coefficients χ_1 and χ_2 set equal to zero. Then

$$M \frac{d^2 \beta_{n\alpha}}{dt^2} - w(\beta_{n+1, \alpha} - 2\beta_{n\alpha} + \beta_{n-1, \alpha}) = 0 \quad (2')$$

This is a linear equation for longitudinal sound propagation on the helix, where $\beta_{n\alpha}$ is the displacement of unit cell n on spine α from its equilibrium position and M is the mass of (see Fig. 1)

$$2C + O + N + H + R$$

For the computations reported here, we (quite arbitrarily) take R to be CH_3 . Thus

$$\begin{aligned} M &= 70 \times \text{mass of proton} \\ &= 1.17 \times 10^{-25} \text{ kg} \end{aligned}$$

The parameter w in Eq. (2') gives the linear restoring force per unit of

*One electron-volt (eV) = $8065.5 \text{ cm}^{-1} = 1.602 \times 10^{-19}$ joule (J).

hydrogen bond stretching. From Ref. 6 a somewhat similar bond is said to have a force constant of 0.76 mdyne/Å.* Thus we take

$$w = 76 \text{ N/m}$$

From Eq. (2') the longitudinal sound speed is $[w/M]^{1/2}$ times the longitudinal distance between unit cells. Since the pitch of the helix is 5.4 Å, corresponding to 3.6 spines, the length of a single unit cell along one spine is 4.5 Å. Thus

$$\text{sound speed} = 1.15 \times 10^4 \text{ m/sec}$$

2.4. Dipole–Dipole Coupling

If Eq. (1) is considered in the approximation that the sound energy W and the nonlinear coefficients χ_1 and χ_2 are zero, it can be written in the form

$$i\hbar \frac{da_{n\alpha}}{dt} + J(a_{n-1,\alpha} - 2a_{n\alpha} + a_{n+1,\alpha}) - \mathcal{E}_0 a_{n\alpha} = -2Ja_{n\alpha} + L(a_{n,\alpha+1} + a_{n,\alpha-1}) \quad (1'')$$

These terms with coefficients J and L represent the effects of dipole–dipole couplings between the amide-I vibrations. The particular form presented in Eq. (1'') emphasizes that the effect of the “ J -term” is to provide a mechanism for longitudinal propagation of bond energy. Indeed if the left-hand side of Eq. (1'') were zero, it would be satisfied by a plane wave of probability amplitude propagating in a dispersive manner.

The “ J -term” represents dipole–dipole coupling between a particular amide-I bond and its next neighbors in the longitudinal direction. The “ L -term” represents a corresponding coupling to lateral neighbors. Fortunately for our numerical studies, the values for these coupling coefficients have been calculated (and checked for their effects on infrared spectra) as⁵:

$$J = 7.8 \text{ cm}^{-1} = 1.55 \times 10^{-22} \text{ J}$$

and

$$L = 12.4 \text{ cm}^{-1} = 2.46 \times 10^{-22} \text{ J}$$

2.5. Nonlinear Coefficients χ_1 and χ_2

The nonlinear coefficients χ_1 and χ_2 represent anharmonicity in the longitudinal hydrogen bonds. Their effect is to provide nonlinear coupling between the longitudinal sound waves Eq. (2') and dispersive propagation of amide-I bond

*One dyne = 10^{-5} newton (N).

energy Eq. (1'') as was described in Section 1. This coupling permits the formation of a soliton.

To be more specific, note in Eq. (2) that the " χ -terms" act as a source for the longitudinal sound. Once generated, this sound energy acts in Eq. (1) as a "potential well" for the bond energy, which prevents its dispersion.

Some information on the level of anharmonicity in the hydrogen bonds of α -helix protein is available in Ref. 7. For the purpose of our numerical studies, we have assumed

$$\chi_1 = \chi_2 \equiv \chi \quad (4)$$

and allowed χ to be an adjustable parameter. Rough estimates, outlined in Appendix B, however, indicated that

$$\chi \sim 2-6 \times 10^{-11} \text{ N}$$

2.6. Sound Energy W

The total longitudinal sound energy is defined as W in Eq. (3) and enters as an additional energetic term in Eq. (1). Including it to the approximation described by Eq. (1') indicates that its effect is merely to speed the rate of phase advance by a small amount. The numerical effect of this term in our results is negligible.

3. NUMERICAL OBSERVATIONS

Equations (1)–(3) contain too many physical constants for a convenient numerical study. Thus the equations we have actually computed are written in the normalized form.

$$\begin{aligned} i \frac{dA_{n\alpha}}{d\tau} = & 1.41 A_{n\alpha} \sum_{n\alpha} \left[\left(\frac{dB_{n\alpha}}{d\tau} \right)^2 + (B_{n\alpha} - B_{n-1,\alpha})^2 \right] \\ & - 0.058(A_{n-1,\alpha} + A_{n+1,\alpha}) + 0.092(A_{n,\alpha+1} + A_{n,\alpha-1}) \\ & + 0.372 \times (10^{10} \chi) [B_{n+1,\alpha} - B_{n-1,\alpha}] A_{n\alpha} \\ & + B_{n+1,\alpha} A_{n+1,\alpha} - B_{n-1,\alpha} A_{n-1,\alpha} - B_{n\alpha} (A_{n+1,\alpha} - A_{n-1,\alpha}) \end{aligned} \quad (1''')$$

$$\begin{aligned} \frac{d^2 B_{n\alpha}}{d\tau^2} - (B_{n+1,\alpha} - 2B_{n\alpha} + B_{n-1,\alpha}) = & 0.132(10^{10} \chi) \\ & \times [|A_{n+1,\alpha}|^2 - |A_{n-1,\alpha}|^2] \\ & + A_{n\alpha}^* (A_{n+1,\alpha} - A_{n-1,\alpha}) + (A_{n+1,\alpha}^* - A_{n-1,\alpha}^*) A_{n\alpha} \end{aligned} \quad (2'')$$

In these equations:

$$a_{n\alpha} \equiv A_{n\alpha} \exp\left(\frac{-i\mathcal{E}_0 t}{\hbar}\right) \quad (5a)$$

$$\beta_{n\alpha} \equiv B_{n\alpha} \times 10^{-11} \text{ m} \quad (5b)$$

$$\tau \equiv t \left(\frac{w}{M}\right)^{1/2} \quad (5c)$$

where we note that Eq. (5a) absorbs the fast phase advance in amide-I bond amplitude, Eq. (5b) measures displacement in units of 0.1 Å, and (5c) measures time in units of

$$\left(\frac{M}{w}\right)^{1/2} = 3.92 \times 10^{-14} \text{ sec}$$

This is the natural period of longitudinal sound vibration (divided by 2π). From Eq. (2'') it can be seen that the longitudinal sound velocity is unity in these units.

We take the total number of unit cells

$$n_{\max} = 200$$

Since, as previously mentioned, the length of a single unit cell along a spine is 4.5 Å, this corresponds to a total length of 900 Å: about the length of a typical myosin molecule in a thick fiber of striated muscle.

As initial conditions we write

$$A_{n\alpha} = 1 \quad \text{for } n = 1$$

$$A_{n\alpha} = 0 \quad \text{for } n \neq 1$$

and

$$B_{n\alpha} = 0 \quad \text{for all } n$$

at $\tau = 0$. Physically this corresponds to the introduction of one quantum of amide-I bond energy onto each of the three spines to excite what Davydov has called the symmetric mode.

The only item remaining to be specified in Eqs. (1''') and (2'') is χ , the level of anharmonicity in the hydrogen bond. Guided by our previously mentioned estimates (see Appendix B), we choose $\chi = 10^{-11}$ N. The calculations are displayed in Fig. 2 where

$$U(1) \equiv A_{n_1}^2 + A_{n_2}^2 + A_{n_3}^2$$

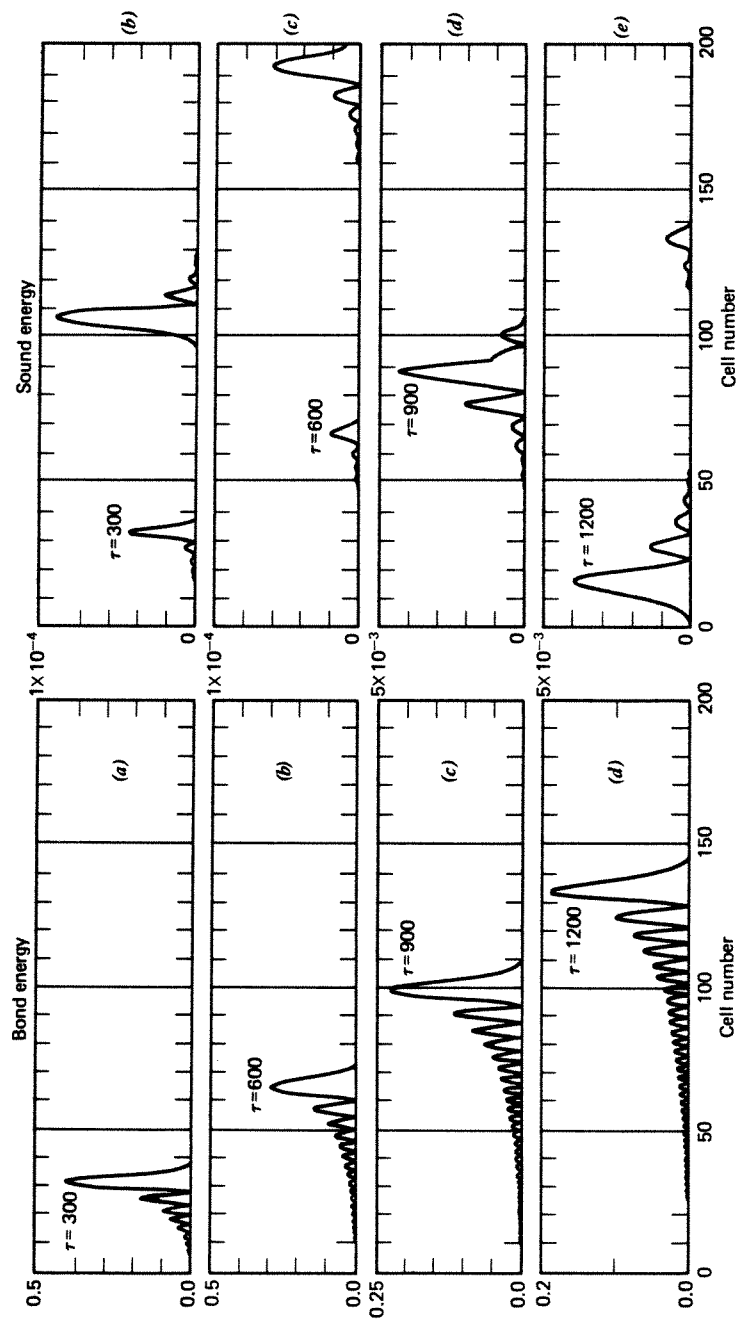


Figure 2. Symmetric three-spine excitation at $\chi = 10^{-11} \text{ N}$.

and

$$U(2) \equiv \sum_{\alpha} \left[\left(\frac{dB_{n\alpha}}{d\tau} \right)^2 + (B_{n+1,\alpha} - B_{n,\alpha})^2 \right]$$

Consider first the result for $\tau = 300$ (Fig. 2*a*). The bond energy $U(1)$ has dispersed somewhat and is moving away from the point of initiation at a normalized speed of about 0.1. The longitudinal sound energy $U(2)$ consists of two distinct components: a "fast" component traveling at the limiting sound speed and therefore found at $n = 100$, and a "slow" component that is locked to the bond energy. Does the interaction of bond energy and slow sound constitute of soliton? Figures 2*a* ($\tau = 300$), 2*b* ($\tau = 600$), 2*c* ($\tau = 900$), and 2*d* ($\tau = 1200$), indicate that the bond energy does *not* settle into the hyperbolic secant shape that characterizes a soliton.² On the contrary, it continues to disperse until at $\tau = 1500$ (Fig. 2*f*) it has spread itself over half the molecule.

To see how the bond energy dispersion at $\chi = 10^{-11}$ N differs from linear dispersion, turn to Fig. 3, where the computation is repeated for the case $\chi = 0$. Note that the linear bond dispersions at $\tau = 600$ (Fig. 3*a*) and at $\tau = 900$ (Fig. 3*b*) are *identical* to those in Figs. 2*c* and 2*d*. Thus we must conclude that nonlinear coupling between amide-I energy and sound energy plays no role in the computations of Fig. 2. The threshold level has not been attained; solitons have not formed.

If the nonlinearity parameter is raised an order of magnitude, to the level $\chi = 10^{-10}$ N, the dynamic behavior of the bond energy is strikingly different. As Fig. 4 clearly shows, it no longer disperses but propagates along the helix with a fixed shape and a normalized velocity of 0.132. In this case the level of

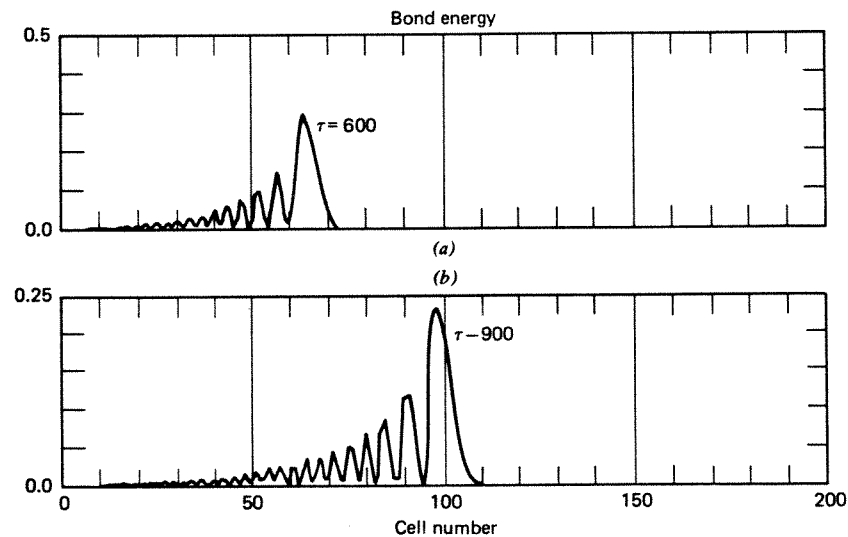


Figure 3. Symmetrical three-spine excitation at $\chi = 0$.

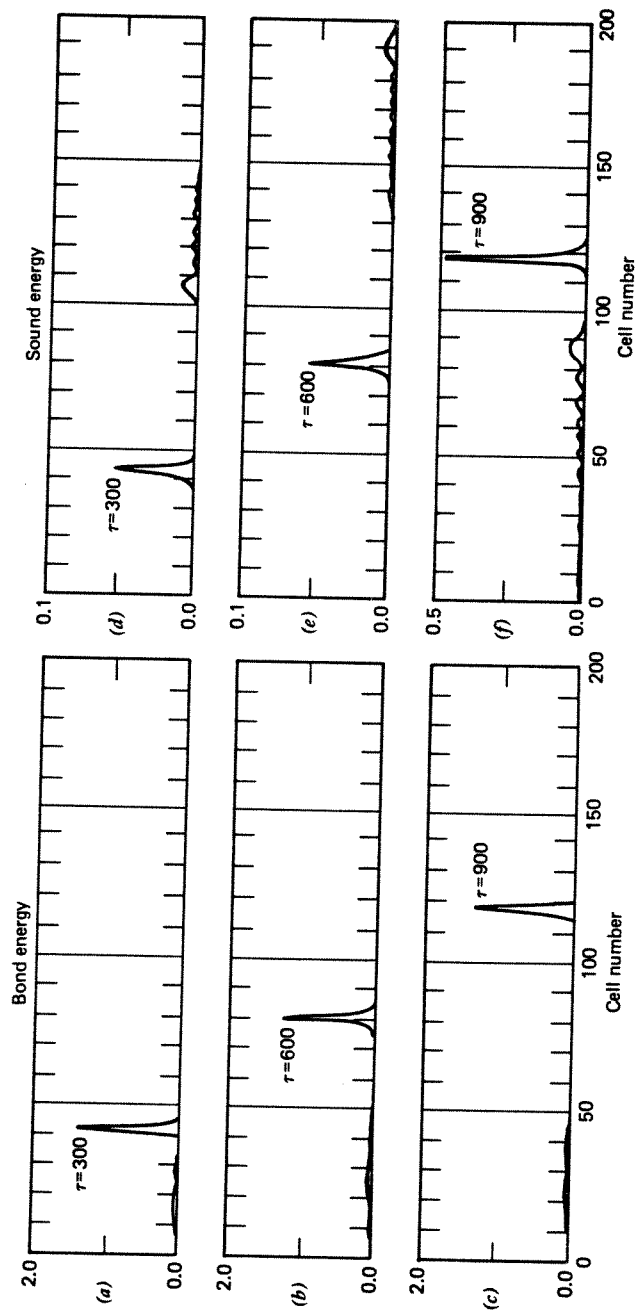


Figure 4. Symmetrical three-spine excitation at $\chi = 10^{-10}$ N.

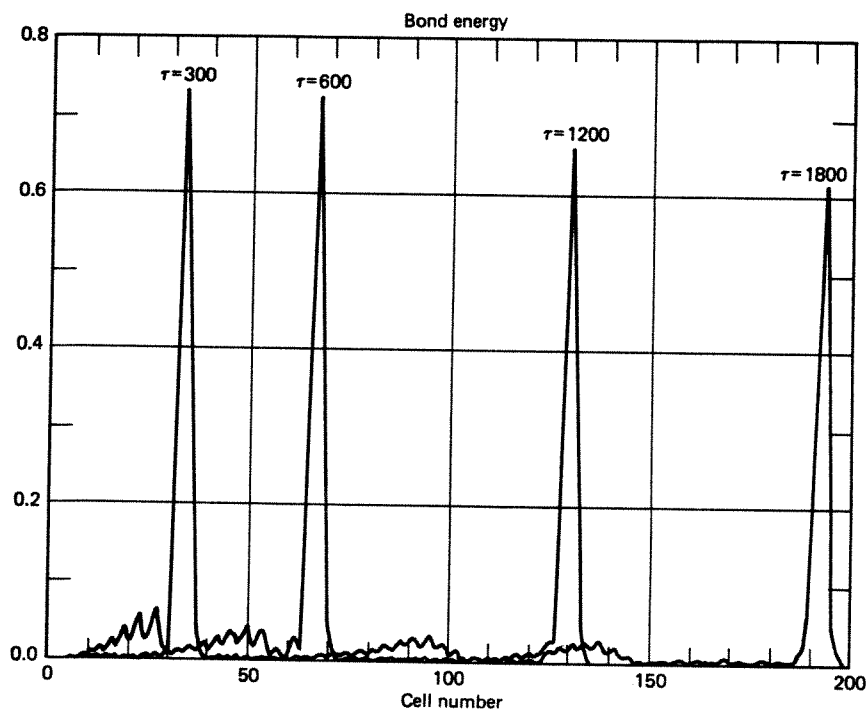


Figure 6. Symmetrical three-spine excitation at $\chi = 5 \times 10^{-11}$ N.

configuration. To illustrate this effect Fig. 8 plots the peak bond energy in the excited spine and that in one of the unexcited spines as a function τ .

Finally we consider the influence of single-spine excitation upon the threshold for soliton formation. For $\chi = 5 \times 10^{-11}$ N the appropriate data are presented in Fig. 9, which shows that a soliton does not develop; rather, the packet of bond energy emits "bursts" of longitudinal sound. If, however, the nonlinear parameter is raised to $\chi = 7 \times 10^{-11}$ N, the data of Fig. 10 clearly show the development of a soliton.

4. MECHANICAL BENDING OF THE HELIX

Davydov has suggested that one effect of soliton propagation along an α -helix might be to cause a mechanical bend (kink?) of the helix.² Such an effect would not appear for the symmetric (or three-spine) solitons described in Section 3 because each spine would be elongated equally. However the system composed of Eqs. (1'') and (2'') can also support an antisymmetric soliton for which

$$\begin{aligned} A_{n1} &= -A_{n2} \\ A_{n3} &= 0 \end{aligned}$$

Since the longitudinal sound is insensitive to the phase of $A_{n\alpha}$, this mode would elongate spines 1 and 2 but would leave spine 3 unchanged.

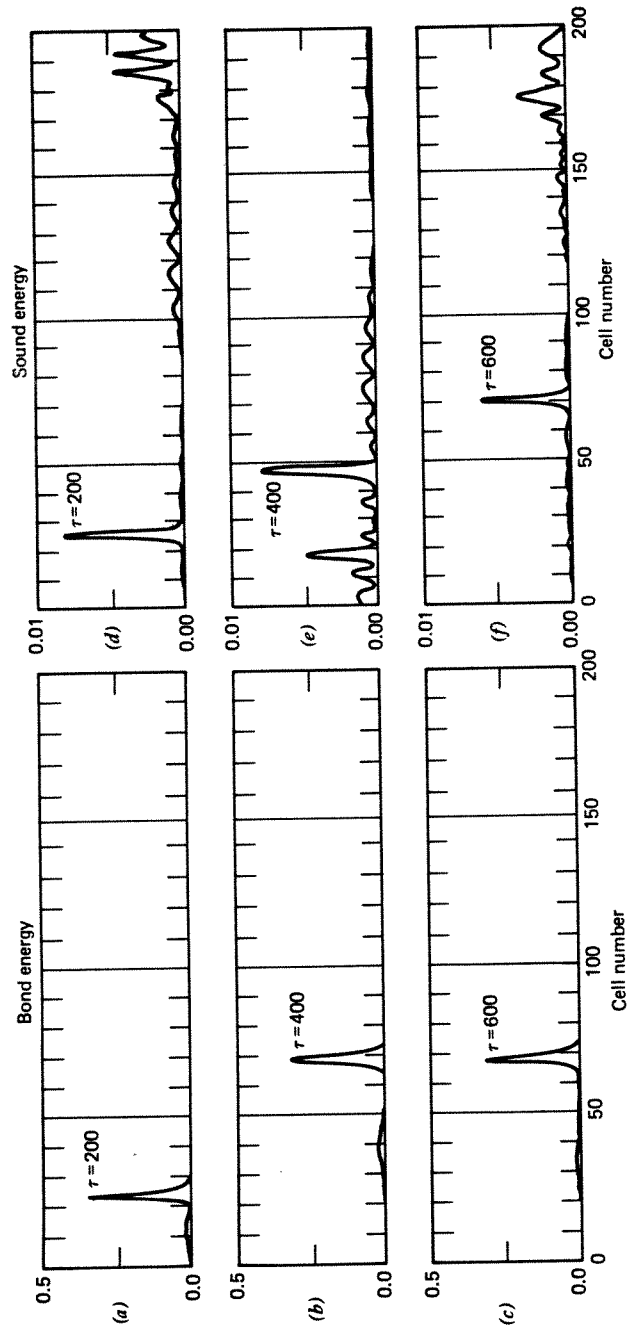


Figure 7. Single-spine excitation at $\chi = 10^{-10} \text{ N}$.

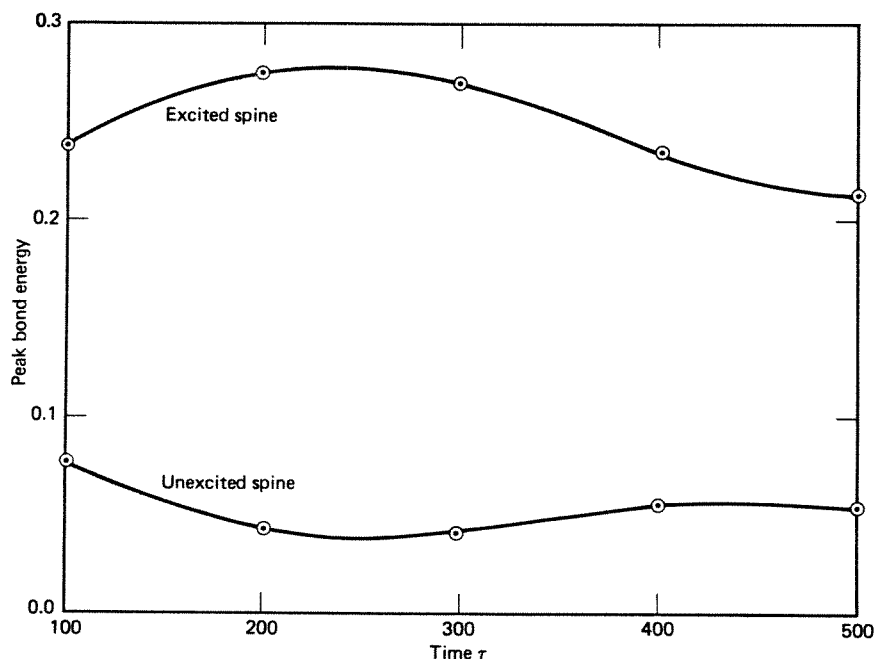


Figure 8. Bond energy in excited spine and unexcited spine versus time for single-spine excitation with $\chi = 10^{-10} N$.

The amount of such elongation is readily computed from the results developed in Appendix A. From Eq. (A2) we have

$$\rho = 0.264 \frac{10^{10} \chi}{1 - s^2} |A|^2$$

and the total elongation is

$$\begin{aligned} \int \rho d\xi &= 0.264 \frac{(10^{10} \chi)}{1 - s^2} \int A^2 d\xi \\ &= 0.264 \frac{(10^{10} \chi)}{1 - s^2} \end{aligned} \quad (7)$$

where N is the total number of amide-I quanta being carried along a single spine by the soliton and s is the soliton speed.

Since the radius of α -helix is 2.8 \AA , the turning radius for the bend is $(1 + \sqrt{3}/2)2.8 = 5.23 \text{ \AA}$. Also the right-hand side of Eq. (7) is in units of 0.1 \AA [see Eq. (5b)]. Thus the angle (θ) of the bend will be

$$\theta = \tan^{-1} \left[0.00505 N \frac{10^{10} \chi}{1 - s^2} \right]$$

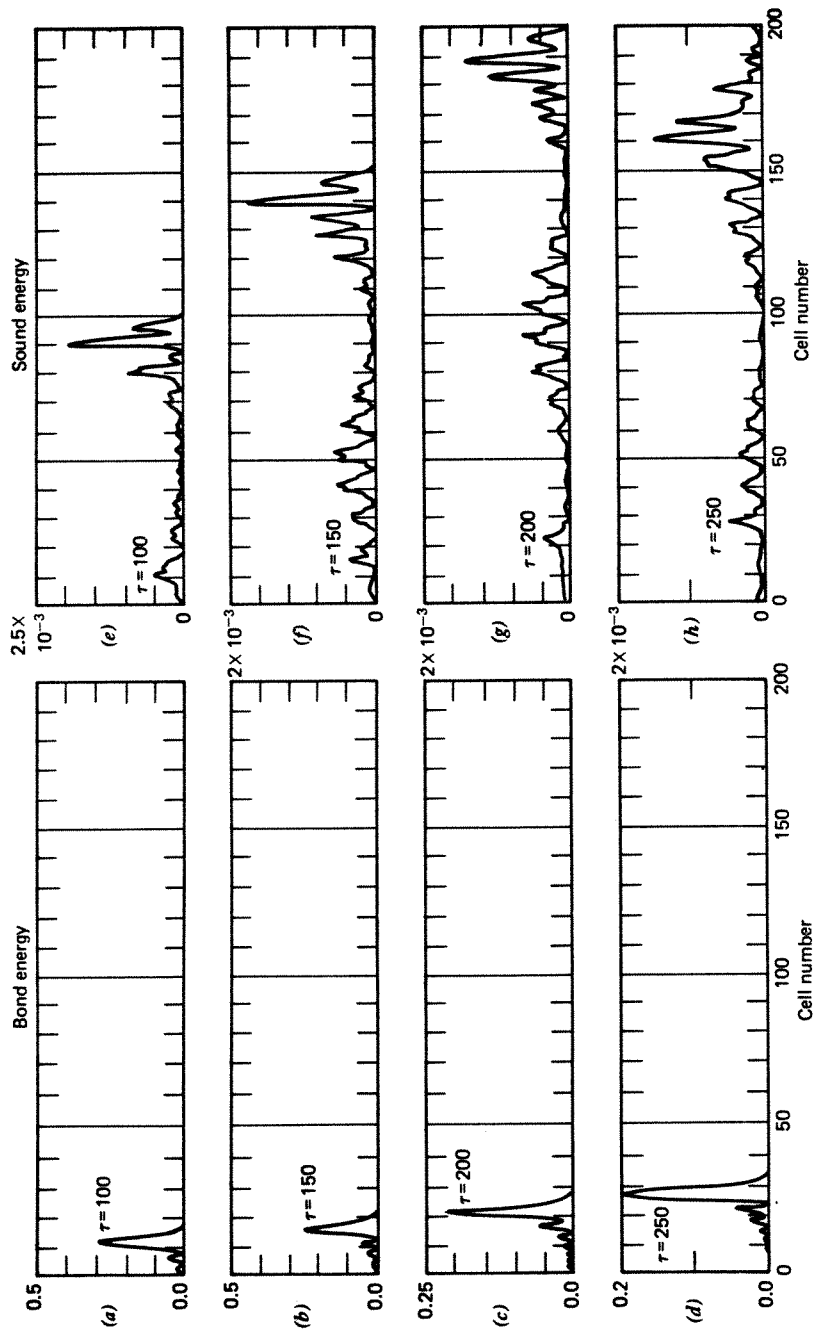


Figure 9. Single-spine excitation at $x = 5 \times 10^{-11}$ N.

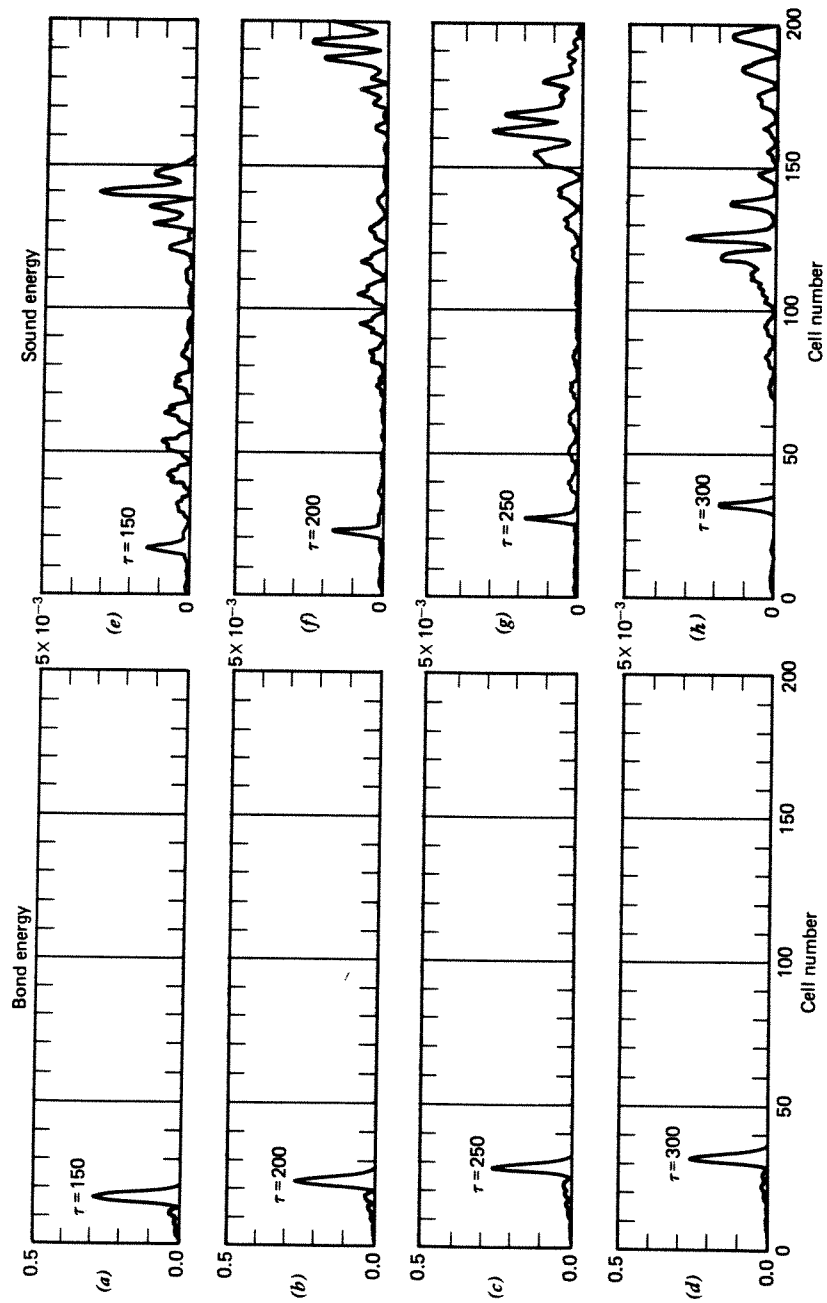


Figure 10. Single-spine excitation at $\chi = 7 \times 10^{-11}$ N.

To a good approximation, therefore, the angle of bend will be

$$\theta \doteq 0.29N(10^{10}\chi) \text{ deg} \quad (8)$$

The same angle of bend would be observed for N quanta propagating along a single spine. However, as we noted in connection with the single-spine computations presented in Figs. 7 and 9, such an excitation tends to relax into the symmetric mode.

5. SUMMARY OF RESULTS

5.1. Threshold for Soliton Formation

Our numerical and analytical studies show that with symmetrical (three-spine) excitation of the initial cell, the threshold level of nonlinearity for soliton formation is

$$\chi > \frac{3}{N} \times 10^{-11} \text{ N}$$

where N is the number of amide-I quanta introduced onto each spine. Comparing this result with our order estimates

$$\chi > 2 - 6 \times 10^{-11} \text{ N}$$

for the nonlinear parameter, we see a possibility of soliton formation with a single quantum on each spine. As the number of quanta introduced becomes larger, the likelihood of soliton formation increases. In this connection it is important to note that the 0.5 eV released in each event of ATP hydrolysis is more than enough to introduce two quanta into an amide-I bond.

5.2. Soliton Speed

From both numerical computations and analytical calculations we find the soliton speed near threshold to be almost equal to the group velocity of a linear pulse below threshold. From our numerical computations it is 0.11 of longitudinal sound speed or

$$\text{soliton speed} \sim 1.26 \times 10^3 \text{ m/sec}$$

Thus the time required for a soliton to traverse 1000 Å (about the length of a typical myosin molecule in striated muscle) is about 80 psec.

5.3. Mechanical Bending

The mechanical bending of the α -helix under symmetrical excitation is zero, but if the soliton is antisymmetric (in the sense defined by Davydov) or if all the bond energy is confined to a single spine, the bend angle is approximately $\theta = 0.45N(10^{10}\chi)$. This could be a significant effect for several amide-I quanta

in the soliton and a nonlinear parameter somewhat larger than the values estimated in Appendix B.

6. OPEN QUESTIONS

In an exploratory study such as this it is as important to indicate what we have *not* shown as it is to itemize our results. Davydov has clearly changed the question posed at the beginning of this chapter to: "Is biological energy transmitted by solitons?" A definitive answer is not yet available, however. Indeed it is rather exciting to await future scientific developments that should indicate whether the *real* level of nonlinearity in a α -helix is approximately that estimated in Appendix B (indicating that solitons should easily form at the single quantum level), or substantially smaller (indicating that several quanta must participate to form a soliton). We feel that the following questions should be given high priority.

1. *Additional Numerical Studies.* The numerical studies presented here are not complete, and additional investigations should include the following: (a) a more careful study of relaxation from single-spine excitation, (b) more general initial conditions, to initialize more than one cell and to excite Davydov's antisymmetric mode, (c) inclusion of additional dipole-dipole coupling terms from Ref. 5, (d) augmentation of Davydov's equations to include additional degrees of freedom, and (e) study of soliton propagation through a nonuniform α -helix.

2. *The Level of Anharmonicity.* Every effort should be given to obtain better experimental measurements and theoretical estimates of the anharmonicity (χ) in the hydrogen bonds of α -helix protein. We have not found really satisfactory estimates from the literature⁷ and present the order estimates of Appendix B as a rough guide. But we are not biochemists (nor chemists, even) so relevant information may be lying about. The level of anharmonicity is the most important fact in nonlinear biomolecular dynamics.

ACKNOWLEDGMENTS

It is a pleasure to thank Profs. A. S. Davydov, C. Sandorfy, and D. E. Green for stimulating private discussions of this problem and Prof. M. Sundaralingam for several interesting comments on the structure of α -helix protein.

APPENDIX A: THE INITIAL VALUE PROBLEM IN LINEAR AND NONLINEAR LIMITS

The original difference-differential equations, Eqs. (1''') and (2''), are approximated as partial differential equations and studied analytically. In the linear limit, a Fourier transform solution is discussed. In the nonlinear limit,

the inverse scattering transform⁸ is used to find the threshold for soliton creation and soliton speed.

From the numerical results presented above, it is evident that several unit cells participate in the structure of each soliton. Thus, as Davydov et al. have shown,⁴ Eqs. (1''') and (2'') can be approximated as

$$i \frac{\partial A}{\partial \tau} + 0.058 \frac{\partial^2 A}{\partial \xi^2} - F(\tau)A \doteq 0.744(10^{10}\chi)\rho A \quad (\text{A1})$$

$$\frac{\partial^2 \rho}{\partial \tau^2} - \frac{\partial^2 \rho}{\partial \xi^2} \doteq + 0.264(10^{10}\chi) \frac{\partial^2}{\partial \xi^2} |A|^2 \quad (\text{A2})$$

where ξ is a continuous variable approximating the longitudinal index n . Also

$$\rho \equiv - \frac{\partial B}{\partial \xi}$$

and

$$F(\tau) \equiv 0.068 + 1.41 \sum_{\alpha} \int \left[\left(\frac{\partial B_{\alpha}}{\partial \tau} \right)^2 + \left(\frac{\partial B_{\alpha}}{\partial \xi} \right)^2 \right] d\xi$$

The term $F(\tau)A$ can be eliminated from Eq. (A1) by adjusting the phase of A as

$$A = \mathcal{Q} \exp \left[-i \int^{\tau} F(\tau') d\tau' \right]$$

The numerical results also show that soliton speed is slow compared with sound speed. Thus Eq. (A2) becomes approximately

$$\rho = \frac{0.264(10^{10}\chi)}{1-s^2} |\mathcal{Q}|^2 \quad (\text{A3})$$

where s is the wave speed. With these approximations, Eq. (A1) takes the form

$$i \frac{\partial \mathcal{Q}}{\partial \tau} + 0.058 \frac{\partial^2 \mathcal{Q}}{\partial \xi^2} = - \frac{0.196(10^{10}\chi)^2}{1-s^2} |\mathcal{Q}|^2 \mathcal{Q} \quad (\text{A4})$$

This is the "nonlinear Schrödinger equation," which has been exactly solved by Zakharov and Shabat for arbitrary initial conditions.⁹

We are interested in the initial conditions (Fig. A1)

$$\begin{aligned} A &= \frac{N}{p} && \text{for } 0 < \xi < p \\ &= -\frac{N}{p} && \text{for } -p < \xi < 0 \\ &= 0 && \text{for } |\xi| > p \end{aligned}$$

These initial conditions deserve a word of explanation (Fig. A2). In our numerical computations a certain number (N) of amide-I quanta were put

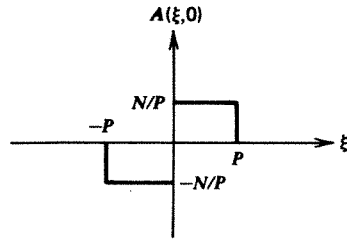


Figure A1. Initial conditions.

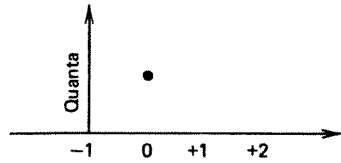


Figure A2.

onto the $n = 0$ bond at time $\tau = 0$. All other amide-I bonds were without energy at $\tau = 0$ and the energy at $n = -1$ was maintained at the value zero throughout the computations. An antisymmetrical form is chosen for the full line ($-\infty < \xi < +\infty$) to maintain the boundary condition of zero at the origin ($n = -1$). We have no precise value for p , but it should be approximately 2.

For analysis it is convenient to normalize Eq. (A4) by writing

$$\mathcal{Q} = 3.19 \frac{(1 - s^2)^{1/2}}{(10^{10} \chi)} \phi$$

$$\xi = 0.241x$$

$$\tau = t$$

Then Eq. (A4) takes the form*

$$i\phi_t + \phi_{xx} = -2|\phi|^2\phi \tag{A4'}$$

with the initial conditions

$$\begin{aligned} \phi &= \frac{(10^{10} \chi)N}{3.19p(1 - s^2)^{1/2}} && \text{for } 0 < x < p/0.241 \\ &= -\frac{(10^{10} \chi)N}{3.19p(1 - s^2)^{1/2}} && \text{for } -p/0.241 < x < 0 \\ &= 0 && \text{for } |x| > p/0.241 \end{aligned}$$

*Subscripts are used to indicate partial differentiation.

A.1. Linear Limit

When the amplitude in Eq. (A4') is small enough so the nonlinear term ($|\phi|^2\phi$) can be neglected, it becomes simply $i\phi_t + \phi_{xx} = 0$ with the Fourier transform solution

$$\phi(x, t) \approx \int_{-\infty}^{\infty} \frac{\sin^2(k\bar{p}/2)}{(k\bar{p}/2)} \exp[i(kx - k^2t)] dk \quad (\text{A5})$$

where

$$\bar{p} \equiv \frac{p}{0.241}$$

The integrand in Eq. (A5) takes its maximum value when k is the root of $\tan(k\bar{p}/2) = k\bar{p}$ or

$$k_{\max} = \frac{2.331\dots}{\bar{p}}$$

and the corresponding group velocity [where the phase $(kx - k^2t)$ is stationary] is $2k_{\max}$. Thus the linear pulse velocity (in unnormalized units that correspond to the numerical computations) is

$$\text{linear pulse velocity} = \frac{0.271}{p} \quad (\text{A6})$$

For $p = 2$ this implies a linear pulse velocity of 0.135 whereas from the numerical computations displayed in Fig. 3 we find a velocity of 0.11.

The amplitude in Eq. (A5) should fall asymptotically as $t^{-1/2}$, indicating that the maximum bond energy in the linear limit should fall as $1/\tau$.¹⁰ This in turn implies that the bond energy must "spread out" over a length of the α -helix that is proportional to τ . Such an effect is observed in the data of Figs. 2 and 5.

A.2. Soliton Limit

We now use the analytical tools of the inverse scattering transform method to find the threshold for soliton formation and its corresponding velocity. Readers are forewarned that this discussion will be completely unintelligible unless they have some working knowledge of the inverse scattering transform method. Those who do not should merely note that it is a generalization of the Fourier transform method.⁸

For the Zakharov–Shabat linear scattering operator⁹

$$i \begin{bmatrix} \partial_x & -\phi \\ -\phi & -\partial_x \end{bmatrix} \begin{bmatrix} \psi_1 \\ \psi_2 \end{bmatrix} = \gamma \begin{bmatrix} \psi_1 \\ \psi_2 \end{bmatrix}$$

and the initial conditions listed in Eq. (A4'), we assume asymptotic scattering amplitudes at $t = 0$ to be

$$\begin{bmatrix} \psi_1 \\ \psi_2 \end{bmatrix} = \begin{bmatrix} 1 \\ 0 \end{bmatrix} \exp(-i\gamma x) \quad \text{for } x < -p$$

and

$$\begin{bmatrix} \psi_1 \\ \psi_2 \end{bmatrix} = a(\gamma) \begin{bmatrix} 1 \\ 0 \end{bmatrix} \exp(-i\gamma x) + b(\gamma) \begin{bmatrix} 0 \\ 1 \end{bmatrix} \exp(+i\gamma x) \quad \text{for } x > p$$

Then we find

$$a(\gamma) = \exp(2i\gamma\bar{p}) \left[\left(\cos m\bar{p} - \frac{i\gamma}{m} \sin m\bar{p} \right)^2 + \frac{K^2}{(m\bar{p})^2} \sin^2 m\bar{p} \right] \quad (\text{A7})$$

where

$$m^2 \equiv \gamma^2 + \frac{K^2}{\bar{p}^2}$$

$$\bar{p} \equiv \frac{p}{0.241}$$

$$K \equiv \frac{(10^{10}\chi)N}{0.241 \times 3.19(1-s^2)^{1/2}}$$

Solitons correspond to zeros of Eq. (A7) that lie in the upper half of the γ -plane. For such a zero at $\gamma = \gamma_r + i\gamma_i$, the corresponding soliton has⁸

$$\text{speed} = 4\gamma_r$$

$$\text{amplitude} = 2\gamma_i$$

For K small (i.e., as $\chi \rightarrow 0$), $a(\gamma)$ has no upper half-plane zeros. Thus the threshold for soliton formation occurs when the first zero Eq. (A7) crosses the real axis of the γ -plane. Since a zero of Eq. (A7) implies

$$\cot(m\bar{p}) = i \left(\frac{\gamma\bar{p} \pm K}{m\bar{p}} \right)$$

a real axis zero can only occur where $\cot(m\bar{p}) = 0$ or at

$$\pm\gamma_r\bar{p} = K = \frac{\pi}{2\sqrt{2}}$$

For units that correspond to the numerical computations, the threshold condition is for $s = 0.11$)

$$\chi N > 7.64 \times 10^{-11} \text{ N} \quad (\text{A8})$$

This threshold level is higher than that in Eq. (6).

The soliton velocity at threshold (again in units that correspond to the numerical computations) is

$$\text{soliton velocity} = \frac{0.258}{p} \quad (\text{A9})$$

Comparison with Eq. (A6) shows that the soliton velocity at threshold should be quite close (i.e., within 5%) to the linear pulse velocity. This is confirmed by the numerical data of Figs. 5 and 6 (particularly 5c and 6d).

We note finally that solitary wave solutions of the set composed of Eqs. (A1) and (A2) have been studied rather extensively in plasma physics, where they are called "Langmuir solitons." Reference 11 is a particularly lucid introduction to this work.

APPENDIX B: ORDER ESTIMATES OF HYDROGEN BOND NONLINEARITY

This appendix obtains order of magnitude estimates for the level of anharmonicity to be expected in longitudinal vibrations of α -helix protein. The hydrogen bond is assumed to have the anharmonic potential (about the minimum at x_0)

$$U(x) = \frac{1}{2}wx^2 + ax^3 \quad (\text{B1})$$

Nonlinearity enters Davydov's Hamiltonian formalism as an "interaction" term

$$H_{\text{int}} = \chi B^\dagger B x \quad (\text{B2})$$

where $B^\dagger B$ gives the number of quanta in the amide-I bond. If the restoring force of this bond is taken to be $K \text{ N/m}$, the bond extension is

$$B^\dagger B \hbar \omega_0 = \frac{1}{2} K x^2 \quad (\text{B3})$$

where

$$\hbar \omega_0 = \mathcal{E}_0 = 0.328 \times 10^{-19} \text{ J}$$

the quantum energy of an amide-I vibration. From Eqs. (B1)–(B3)

$$\chi = \frac{2 \hbar^2 a}{\mathcal{E}_0 M_r} \quad (\text{B4})$$

where the "reduced mass" of amide-I is

$$\begin{aligned} M_r &= \frac{48}{7} \times \text{mass of proton} \\ &= 1.15 \times 10^{-26} \text{ kg} \end{aligned}$$

To estimate the parameter a in Eq. (B1) we note, from Pauling et al.,¹² that the binding energy of a hydrogen bond in α -helix protein is about 8 kcal/mole or

$$\Delta U = 5.5 \times 10^{-20} \text{ J}$$

But from Eq. (B1) we find (Fig. B1) that $\Delta U = w^3/54a^2$ so

$$\begin{aligned} a &= \frac{w^{3/2}}{\sqrt{54 \Delta U}} \\ &= 38.3 \times 10^{10} \text{ N/m}^2 \end{aligned}$$

Thus from Eq. (B4) we obtain the order estimate

$$\chi \sim 2 \times 10^{-11} \text{ N}$$

We expect the readers to be as suspicious of this estimate as we are; thus we turn to Ref. 7. There the potential Eq. (B1) is written in the form

$$U = \frac{1}{2}kq^2 + k_3q^3 \quad (\text{B1}')$$

where

$$q \equiv \frac{x}{\lambda}$$

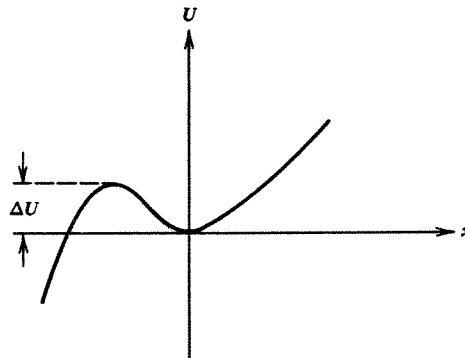


Figure B1. Plot of $\Delta U = w^3/54a^2$.

is a normalized space variable and

$$\lambda \equiv \left[\frac{\hbar}{\omega\mu} \right]^{1/2}$$

in which ω is the radian frequency and μ the reduced mass of the resulting oscillation. Evidently

$$w = \frac{k}{\lambda^2}$$

$$a = \frac{k_3}{\lambda^3}$$

Sandorfy⁷ states: "Model calculations... have shown that k_3 must not exceed 7 or 8% of k ... for [second-order perturbation theory] to be valid. According to our experience this is probably fulfilled for weak hydrogen bonds with ΔU values not higher than about 3 or 4 kcal/mole" (p. 617). Since *our* ΔU is taken to be 8 kcal/mole, it seems reasonable to assume $k_3/k = 0.15$ and to calculate

$$a = \frac{k_3}{k} \frac{w^{5/4} \mu^{1/4}}{\hbar^{1/2}}$$

With μ the reduced mass of an O—N,

$$\mu = \frac{112}{15} \times \text{mass of proton}$$

we find

$$a = 10.96 \times 10^{11} \text{ N/m}^2$$

and therefore

$$\chi \sim 6.3 \times 10^{-11} \text{ N}$$

APPENDIX C: NOTES ON THE NUMERICAL CODE

Equations (1''') and (2'') are solved along three spines ($\alpha = 1, 2, 3$), each containing 201 unit cells ($n_{\max} = 200$). Thus, at each unit cell there are three first-order complex ordinary differential equations Eq. (1''') and three second-order real ordinary differential equations Eq. (2''). These equations are split into a coupled system of 12 first-order real equations at each unit cell to give a total of 2412 ordinary differential equations.

The differential equations were then solved on a CDC 7600 computer using a numerical method of lines code, called PDE1D.¹³ This code integrated the

equations with a third-order Adams–Bashford–Moulton PECE method.¹⁴ The time step was chosen to approximate the solution within a relative error of 0.0001 per unit time interval. For these calculations the time step ranged between 0.15 and 0.5.

The accuracy of the time integration was also checked by rerunning some of the calculations with a much smaller time step. No significant differences were found when these more accurate solutions were compared with the previous calculations.

An independent check on the overall accuracy of each calculation was made by monitoring the total probability

$$P = \sum_{n=0}^{200} \sum_{\alpha=1}^3 A_{n\alpha}^2$$

during the calculation. This probability should remain invariant as $A_{n\alpha}$ evolves according to Eqs. (1''') and (2''). This check remained constant within a few percentage points of its initial value in all the calculations presented here.

APPENDIX D: COMPUTER FILM NOTICE

A computer film illustrating the dynamic effects discussed in this chapter, and in particular the soliton threshold, has been prepared by J. C. Eilbeck, Department of Mathematics, Heriot–Watt University, Edinburgh, Scotland. Under the title “Davydov Solitons,” it is available from Swift Film Productions, 1, Wool Road, Wimbledon, London, SW20 OHN, UK at a price of £55.00.

REFERENCES

1. D. E. Green, “Mechanism of Energy Transduction in Biological Systems,” *Science* **181**, 583–584 (1973). See also *Ann. N.Y. Acad. Sci.* **227** (1974) and, particularly, the “General Discussion” on pp. 108–115.
2. A. S. Davydov, “Solitons in Molecular Systems with Applications in Biology,” *Phys. Scripta* **20** (1979) 387–394. See also *Phys. Stat. Sol.* **75**, 735–742 (1976) and *Stud. Biophys.* **62**, 1–8 (1977).
3. Since the term “soliton” was coined by Zabusky and Kruskal [*Phys. Rev. Lett.* **15**, 240–243 (1965)], thousands of papers have appeared in a wide variety of research areas. Several recent books include: R. Hermann, *The Geometric Theory of Non-linear Differential Equations* (Math Sciences Press, Brookline, MA, 1977); *Solitons in Action*, K. Lonngren and A. Scott, Eds. (Academic Press, New York, 1978); *Solitons in Condensed Matter Physics*, A. R. Bishop and T. Schneider, Eds., Springer-Verlag, New York, (1979); *Solitons*, P. J. Caudry and R. K. Bullough, Eds. (Springer-Verlag, New York, to appear); G. L. Lamb, Jr., *Elements of Soliton Theory* (Wiley-Interscience, New York, to appear).
4. A. S. Davydov, A. A. Eremko, and A. I. Seraienko, “Solitonui b α -Spiralnoi Belkovuix Molekulax,” *Ukr. Fiz. Zh.* **23**, 983–993 (1978).

5. N. A. Nevskaya and Yu. N. Chirgadze, "Infrared Spectra and Resonance Interactions of Amide-I and -II Vibrations of α -Helix," *Biopolymers* **15**, 637-648 (1976).
6. W. C. Hamilton and J. A. Ibers, *Hydrogen Bonding in Solids*, (Benjamin, New York, 1968, p. 164.
7. For recent surveys of anharmonicity in hydrogen bonds see: P. Schuster, G. Zundel, and C. Sandorfy, *The Hydrogen Bond*, Vols. 1-3. (North-Holland, New York, Of particular interest are: Chapter 2 by Schuster, "Energy Surfaces for Hydrogen Bonded Systems," and Chapter 13 by Sandorfy, "Anharmonicity and Hydrogen Bonding."
8. M. J. Ablowitz, D. J. Kaup, A. C. Newell, and H. Segur, "The Inverse Scattering Transform-Fourier Analysis for Nonlinear Problems," *Stud. Appl. Math.* **53**, 249-315 (1974).
9. V. E. Zakharov and A. B. Shabat, "Exact Theory of Two-Dimensional Self-Focusing and One-Dimensional Self Modulation of Waves in Nonlinear Media," *Sov. Phys. [J. Exp. Theor. Phys.* **34**, 62-69 (1972)].
10. See G. B. Whitham, *Linear and Nonlinear Waves* (Wiley-Interscience, New York, 1974), pp. 371-374, for a clear discussion of asymptotic behavior.
11. J. Gibbons, S. G. Thornhill, M. J. Wardrop, and D. ter Haar, "On the Theory of Langmuir Solitons," *J. Plasma Phys.* **17**, part 2, 153-170 (1977).
12. L. Pauling, R. B. Corey, and H. R. Branson, "The Structure of Proteins: Two Hydrogen-Bonded Helical Configurations of the Polypeptide Chain," *Proc. Natl. Acad. Sci.* **37**, 205-211 (1951).
13. D. Durack and J. M. Hyman, "PDEL1B, A Library for the Numerical Solution of Partial Differential Equations," in *Advances in Computer Methods for PDE-III*, R. Vichnevetsky and R. S. Stapleman, Eds. (IMACS, 1979), p. 43.
14. L. S. Shampine and M. K. Gordon, *Computer Solution of Ordinary Differential Equations* (Freeman, San Francisco, 1975).